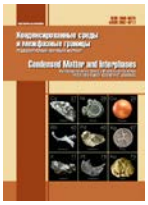

ISSN 1606-867X (Print)
ISSN 2687-0711 (Online)
Condensed Matter and Interphases
Kondensirovannye Sredy i Mezhfaznye Granitsy
https://journals.vsu.ru/kcmf/

Original articles

Research article
https://doi.org/10.17308/kcmf.2021.23/3529

A 3D computer model of the CaO-MgO-Al_2O_3 *T-x-y* diagram at temperatures above 1300 °C

V. P. Vorob'eva, A. E. Zelenaya✉, V. I. Lutsyk, M. V. Lamueva

Institute of Physical Materials Science, Siberian Branch of the Russian Academy of Sciences, 6 Sakhianova ul., Ulan-Ude 670047, Russian Federation

Abstract

The research analyses the controversies surrounding the technique for the formation of a CaO-Al_2O_3 binary system and the nature of melting of compounds in it, i.e. whether the 12:7 compound is technically possible and whether the 1:1 and 1:2 compounds are congruently or incongruently melting compounds. It also discusses whether in the CaO-MgO-Al_2O_3 ternary system the following compounds can be formed: a 3:1:1 compound alone or, in addition to it, two more compounds of 1:2:8 and 2:2:14. A 3D model of the *T-x-y* diagram was created for the most common version, with six binary and three ternary compounds. Its high-temperature portion (above 1300°C) consisted of 234 surfaces and 85 phase regions. Ternary compounds were formed as a result of three peritectic reactions. Besides them, six quasi-peritectic and three eutectic invariant reactions occurred in the system with the participation of the melt. The principle of construction for a three-dimensional model involved a gradual transition from a phase reaction scheme (which is transformed into a scheme of uni- and invariant states) presented in a tabulated and then in a graphical form (a template of ruled surfaces and isothermal planes corresponding to invariant reactions) to a *T-x-y* diagram prototype (graphic images of all liquidus, solidus, and solvus surfaces). The design was concluded with the transformation of the prototype into a 3D model of the real system after the input of the base points coordinates (concentrations and temperatures) and the adjustment of curvatures of lines and surfaces. The finished model provides a wide range of possibilities for the visualisation of the phase diagram, including the construction of any arbitrarily assigned isothermal sections and isopleths. The 3D model was designed with the help of the author's software PD Designer (Phase Diagram Designer). To assess the quality of the 3D model, two versions of an isothermal section at 1840 °C were compared: model section and a fragment of an experimental section near Al_2O_3.

Keywords: Phase diagram, Computer simulation, Oxides of calcium, magnesium, and aluminium

Acknowledgements: The work was carried out in accordance with the state assignment of the Institute of Physical Materials Science, Siberian Branch of the Russian Academy of Science for 2017-2020 (project No. 0336-2019-0008) and was partially supported by the Russian Foundation for Basic Research (project 19-38-90035).

For citation: V. P. Vorob'eva, A. E. Zelenaya, V. I. Lutsyk, M. V. Lamueva. A 3D computer model of the CaO-MgO-Al_2O_3 *T-x-y* diagram at temperatures above 1300 °C. *Kondensirovannye sredy i mezhfaznye granitsy = Condensed Matter and Interphases*. 2021;23(3): 380–386. https://doi.org/10.17308/kcmf.2021.23/3529

Для цитирования: Воробьева В. П., Зеленая А. Э., Луцык В. И., Ламуева М. В. 3D компьютерная модель *T-x-y* диаграммы CaO-MgO-Al_2O_3 при температурах выше 1300 °C. *Конденсированные среды и межфазные границы*. 2021;23(3): 380–386. https://doi.org/10.17308/kcmf.2021.23/3529

✉ Anna E. Zelenaya, e-mail: zel_ann@mail.ru

1. Introduction

The information about phase transformations in the CaO-MgO-Al_2O_3 system, including the subsolidus area, is important for the study of petrological objects, since this system is a component of the CaO-MgO-Al_2O_3-SiO_2 quaternary system which, in its turn, serves as the foundation for the description of deep-seated rock minerals [1–2]. In addition, the prediction and the study of the properties of magnesium aluminate spinel-based cements and technical ceramics are of great importance [3].

Therefore, works dedicated to the experimental study of the CaO-MgO-Al_2O_3 system, thermodynamic calculations, and simulations of its *T-x-y* diagram are of great interest. However, while two of its constituent binary systems, CaO-MgO and MgO-Al_2O_3, have been interpreted unambiguously, there are many controversies in the literature surrounding the third binary system of CaO-Al_2O_3, as well as the ternary system formed by them. As a result, the understanding of the geometric structure of the *T-x-y* diagram, at least with regard to its liquidus surfaces, has been challenged due to many possible interpretations of certain fragments of the diagram.

A spatial (three-dimensional (3D)) computer model of the phase diagram, based at least on one of the most common versions (which can be used to present other simpler versions) can be helpful for the formal description of the T-x-y diagram.

Before constructing the 3D model, it was necessary to redesignate the initial and formed components in the compound system. This is a requirement of the PD Designer software, which was used to construct 3D models of the *T-x-y* phase diagrams [4-6].

Thus, the CaO-MgO-Al_2O_3 system was redesignated as A-B-C.

The binary CaO-MgO (A-B) system is a simple eutectic one [7–9].

According to [10, 11], in the MgO-Al_2O_3 (B-C) binary system a 1:1 or MgO·Al_2O_3 congruently melting compound (designated as R6 in the 3D model) is formed which splits it into an eutectic MgO-MgO·Al_2O_3 (B-R6) and peritectic MgO·Al_2O_3-Al_2O_3 (R6-C) subsystems. What is more, minimums are recorded on the liquidus and solidus lines in the peritectic subsystem.

The structure of the CaO-Al_2O_3 (A-C) system has been debated a lot, the differences relate to the quantity and the nature of the formed compounds and the type of binary dots. For example, [7], with reference to [12], presents a version of the *T-x* diagram where five compounds are formed: the $3CaO·Al_2O_3$ (R1) and $CaO·6Al_2O_3$A (R5) incongruently melting compounds and $12CaO·7Al_2O_3$ (R2), $CaO·Al_2O_3$ (R3), and $CaO·2Al_2O_3$A (R4) congruently melting compounds. Therefore, the system is divided into two eutectic systems: $12CaO·7Al_2O_3$-$CaO·Al_2O_3$ (R2-R3), $CaO·Al_2O_3$-$CaO·2Al_2O_3$ (R3-R4), and two eutectic-peritectic systems: CaO-$12CaO·7Al_2O_3$ (A-R2), $CaO·2Al_2O_3$-Al_2O_3 (R4-C) which are accompanied by the formation of the incongruently melting $3CaO·Al_2O_3$ (R1) and $CaO·6Al_2O_3$ (R5) compounds, respectively. This most complex version of the structure of the CaO-Al_2O_3 (A-C) *T-x* diagram was used to construct a 3D computer model of the *T-x* diagram.

However, according to [13], the $12CaO·7Al_2O_3$ (R2) compound is actually a $Ca_{12}Al_{14}O_{32}(OH)_2$ hydrate and therefore it cannot be found in the CaO-Al_2O_3 system. As a result, instead of five compounds there are four compounds (without $12CaO·7Al_2O_3$) in the system. What is more, the nature of melting of $CaO·Al_2O_3$ (R3), $CaO·2Al_2O_3$ (R4) is also considered to be incongruent, similar to the $3CaO·Al_2O_3$ (R1) and $CaO·6Al_2O_3$ (R5) compounds. In this case, these four compounds are formed as a result of peritectic reactions. Moreover, $3CaO_3·Al_2O_3$ (R1) and $CaO·Al_2O_3$ (R3) interact as a result of an eutectic reaction. The same version of the T-x diagram structure was generated as a result of thermodynamic calculations [14, 15], and was confirmed by the latest experimental research [16].

Based on the published data analysis, [8, 9, 17–19] claimed that the versions of the CaO-Al_2O_3 structure dependent on humidity and the concentration of oxygen in the furnace atmosphere. Depending on this, the $5CaO·3Al_2O_3$ stoichiometry can be attributed to the $12CaO·7Al_2O_3$ compound. According to this version of the phase diagram structure, only one compound, $12CaO·7Al_2O_3$ (R2), melts congruently, while the remaining four, $3CaO·Al_2O_3$ (R1), $CaO·Al_2O_3$ (R3), $CaO·2Al_2O_3$ (R4), and $CaO·6Al_2O_3$ (R5), melt incongruently as a result

of four peritectic reactions. The $12CaO{\cdot}7Al_2O_3$ (R2) compound interacts with the $3CaO{\cdot}Al_2O_3$ (R1) and $CaO{\cdot}Al_2O_3$ (R3) as a result of two eutectic reactions. More recent thermodynamic calculations regarding the CaO-Al_2O_3 system [20] confirm this version of the phase diagram structure. Additionally, the authors emphasised that earlier thermodynamic calculations [15] did not consider the $12CaO{\cdot}7Al_2O_3$ phase since it is not strictly anhydrous. In a conventional air humidity and within a temperature range of 950-1350°C, the $12CaO{\cdot}7Al_2O_3$ absorbs a small amount of water (no more than 1.3 wt%) [20].

In cement systems, the $12CaO{\cdot}7Al_2O_3$ compound was regarded as an aluminate phase, in other words, it was considered to be anhydrous and was included in the diagrams [18, 19]. The $12CaO{\cdot}7Al_2O_3$ compound has been found in the form of a natural mineral and has been called meionite [21]. It is of practical importance for the production of dense ceramics [22].

As for the CaO-MgO-Al_2O_3 ternary system, earlier works [23] did not record the formation of ternary compounds. [24] discussed the formation of three ternary compounds: $3CaO{\cdot}MgO{\cdot}Al_2O_3$ (R7), $CaO{\cdot}2MgO{\cdot}8Al_2O_3$ (R8), and $2CaO{\cdot}2MgO{\cdot}14Al_2O_3$ (R9). The thermodynamic calculations [10] did not consider the $C_{12}A_7$ binary compound What is more, the configuration of the internal field of liquidus that corresponds to the $3CaO{\cdot}MgO{\cdot}Al_2O_3$ (R7) compound is characterised by the fact that its boundaries are formed by four invariant points, whereas in [24] this field is triangular in shape.

Therefore, the aim of this work was to construct a 3D computer model of the CaO-MgO-Al_2O_3 *T-x-y* diagram, including all its surfaces: liquidus, solidus, solvus, ruled surfaces, and the horizontal plane corresponding to the invariant transformations in the ternary system up to a temperature of 1300 °C.

2. Modelling

The computer 3D model of the CaO-MgO-Al_2O_3 (A-B-C) *T-x-y* diagram was constructed using the data from [24] considering the formation of six binary compounds: $3CaO{\cdot}Al_2O_3$ (R1), $CaO{\cdot}6Al_2O_3$ (R5) (incongruently melting), $12CaO{\cdot}7Al_2O_3$ (R2), $CaO{\cdot}Al_2O_3$ (R3), $CaO{\cdot}2Al_2O_3$ (R4), $MgO{\cdot}Al_2O_3$ (R6) (congruently melting), and ternary compounds: $3CaO{\cdot}MgO{\cdot}Al_2O_3$ (R7), $CaO{\cdot}2MgO{\cdot}8Al_2O_3$ (R8), $2CaO{\cdot}2MgO{\cdot}14Al_2O_3$ (R9) (Fig. 1).

For a better display and understanding of the geometric structure of the *T-x-y* diagram, first its prototype was constructed in which the base points were spaced for a better visualisation, however, their temperature coordinates were set according to the temperature range (Fig. 1c).

As can be seen from the prototype, the ternary system involved three peritectic reactions leading to the formation of ternary compounds:

P1: L+B+R3→R7, P2: L+R6+R9→R8,
P3: L+R5+R6→R9

six quasi-peritectic:

Q1: L+A→B+R1, Q2: L+R6→B+R3,
Q3: L+R4→R3+R6, Q4: L+R5→R4+R9,
Q5: L+R9→R4+R8, Q6: L+C→R5+R6

and four eutectic:

E1: L→B+R1+R2, E2: L→B+R2+R7,
E3: L→R2+R3+R7, E4: L→R4+R6+R8

invariant reactions. Since the 3D model was designed in a limited temperature range, above 1300 °C, it did not reflect the processes that occurred in the subsolidus.

The prototype can be used to claim that the *T-x-y* diagram consists of 12 liquidus surfaces corresponding to the beginning of crystallisation of the three initial components, 9 compounds (I = A, B, C, R1-R9), and 12 solidus surfaces conjugated with them between which the L+I two-phase regions are found. Each of the 13 complex planes corresponding to the invariant reactions (three peritectic reactions (P), six quasi-peritectic reactions (Q), and four eutectic reactions (E)) are divided into four simplexes. All 24 invariant liquidus lines (Fig. 1d), together with the 48 solidus lines associated with them pair wisely, function as 72 directing curves for the ruled surfaces which form the boundaries for 24 L+I+J three-phase regions. Accordingly, in this high temperature portion of the diagram 24 I+J two-phase regions and 24 conjugated solvus surfaces should be expected. The boundaries for each of these 13 three-phase regions I+J+K without the liquid are represented by three ruled surfaces, the total number of which is 39.

Therefore, the *T-x-y* diagram is formed by 234 surfaces and 85 phase regions (Fig. 1a).

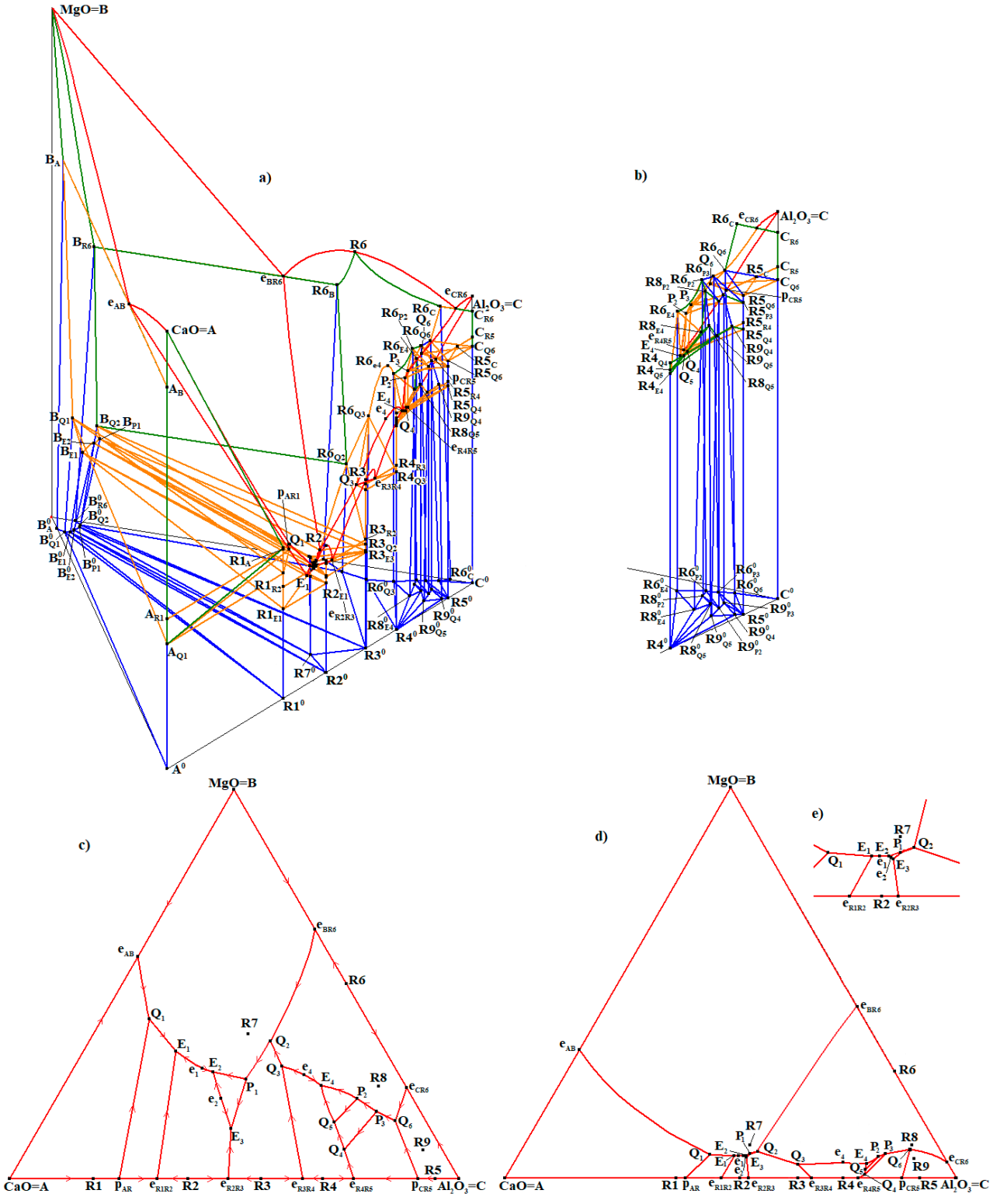

Fig. 1. 3D model of the CaO-MgO-Al_2O_3 (A-B-C) *T-x-y* diagram (a) and an enlarged fragment near Al_2O_3 (b), *x-y* projections of the liquidus surfaces: of the prototype (c), of the real system (d), and its enlarged fragment (e)

3. Results and discussion

The 3D computer model was constructed by assembling the above-mentioned surfaces and phase regions. First, a prototype was formed (Fig. 1b.), i.e. 13 horizontal (isothermal) planes were constructed using the PD Designer: 3 peritectic (P) triangles, 6 quasi-peritectic (Q) quadrangles, 4 triangles which included points E. Then, directing lines were brought to them and ruled surfaces were formed. Thus boundaries for 24 three-phase regions with the melt and 13 solid phase regions were set. The resulting frame was completed with unruled liquidus, solidus, and solvus surfaces.

Next, the prototype was transformed into a 3D model of the phase diagram of the real system. To achieve this, the base points were given real values of concentrations and temperatures and the curvatures of lines and surfaces were adjusted (Fig. 1d).

As a result, a spatial computer model of the *T-x-y* diagram was obtained which has a wide range of visualisation possibilities: the model can be rotated, viewed from arbitrary angles, split into pieces (separate groups of phase regions), arbitrary set sections can also be obtained.

The quality of the resulting model can be assessed by comparing the model sections (Fig. 2a) with the experimental sections (Fig. 2b). The observed isothermal section at 1840 °C is 10 °C lower than the invariant point of the highest temperature Q6 (1850 °C) and higher than point P3 (1830 °C) (Fig. 1a), that is why the crossing traces of the Al_2O_3 phase regions and the melt are not displayed. [24] considered a fragment of the section adjacent to the Al_2O_3 angle, which displayed the section lines limiting the L+R5, L+R6, L+R5+R6, R5, C+R5, R5+R6, C+R5+R6 phase regions (Fig. 2b). The model section was fully calculated and the fragment adjacent to Al_2O_3 was marked (Fig. 2a). Since it was assumed during the construction of the model that the R5 binary compound has a constant composition, the phase regions corresponding to R5 and C+R5 coincided with the edge of the prism, whereas for the spinel R6, on the contrary, a limited solubility was taken into account. Nevertheless, the section topology corresponded to the section presented in [24] (Fig. 2b).

4. Conclusions

A three-dimensional computer model of the CaO-MgO-Al_2O_3 *T-x-y* diagram was constructed.

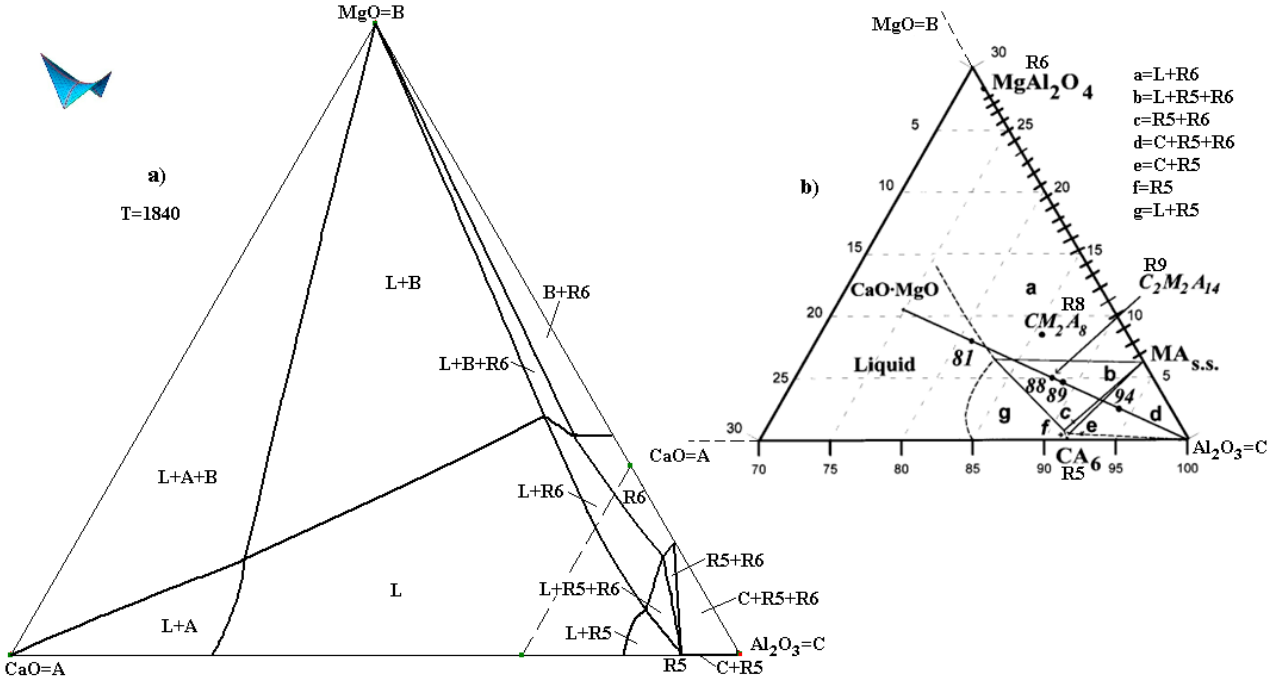

Fig. 2. Isothermal section at 1840°C: 3D models (a), experimentally studied fragment near Al_2O_3 [24] (b) (in [24] the $CaO{\cdot}6Al_2O_3$ (R5) compound has a region of limited solubility, and the $MgO{\cdot}Al_2O_3$ (R6) compound has a region of permanent composition, in 3D models this is vice versa)

It was shown that its high-temperature fragment (above 1300 °C) in the most complex version, i.e. as a result of the formation of six binary: $3CaO{\cdot}Al_2O_3$, $CaO{\cdot}6Al_2O_3$ (incongruently melting), $12CaO{\cdot}7Al_2O_3$, $CaO{\cdot}Al_2O_3$, $CaO{\cdot}2Al_2O_3$, $MgO{\cdot}Al_2O_3$ (congruently melting) and three ternary $3CaO{\cdot}MgO{\cdot}Al_2O_3$, $CaO{\cdot}2MgO{\cdot}8Al_2O_3$, $2CaO{\cdot}2MgO{\cdot}14Al_2O_3$ compounds, it consists of 234 surfaces and 85 phase regions. To assess the quality of the model its sections were compared with the sections constructed using the experimental data.

Author contributions

All authors made an equivalent contribution to the preparation of the publication.

Conflict of interests

The authors declare that they have no known competing financial interests or personal relationships that could have influenced the work reported in this paper.

References

1. Surkov N. V., Gartvich Y. G. Modeling of deep-seated high-alumina parageneses on the basis of the stability fields of corundum- and spinel-normative assemblages of the system CaO-MgO-Al_2O_3-SiO_2. *Russian Geology and Geophysics*. 2012;53(1): 51–61. https://doi.org/10.1016/j.rgg.2011.12.004

2. Banushkina S. V., Gartvich Yu. G., Golitsyna Z. F., Surkov N. V. Experimental study of monovariant melting possibilities in the forsterite-normative part of the CaO-MgO-Al_2O_3-SiO_2 system in connection with the formation of spinel peridotitis. *Mezhdunarodnyy nauchno-issledovatel'skiy zhurnal = International Research Journal*. 2017;66(12): 153–161. https://doi.org/10.23670/IRJ.2017.66.050 (In Russ., abstract in Eng.)

3. Shabanova G. N., Korogodskaya A. N. Physical and chemical bases of spinel cements containing. Part 1. Subsolidus structure of aluminate oxide systems. *Ogneupory i tekhnicheskaya keramika = Refractories and technical ceramics*. 2014;6: 3–7. Available at: https://www.elibrary.ru/item.asp?id=23998838 (In Russ., abstract in Eng.)

4. Lutsyk V. I., Vorob'eva V. P. Computer models of eutectic-type *T–x–y* diagrams with allotropy. *Journal of Thermal Analysis and Calorimetry*. 2010;101(1): 25–31. https://doi.org/10.1007/s10973-010-0855-0

5. Vorob'eva V. P., Zelenaya A. E., Lutsyk V. I., Sineva S. I., Starykh R. V., Novozhilova O. S. High-temperature area of the Fe-Ni-Co-Cu diagram: experimental study and computer design. *Journal of Phase Equilibria and Diffusion*. 2021;42(2): 175-193. https://doi.org/10.1007/s11669-021-00863-3

6. Lutsyk V. I., Zelenaya A. E., Zyryanov A. M. Multicomponent systems simulation by the software of «Diagrams Designer». *Journal Materials, Methods & Technologies. International Scientific Publications*. 2008;2(1): 176–184. Available at: https://www.scientific-publications.net/download/materials-methods-and-technologies-2008.pdf

7. Levin E. M., Robbins C. R., McMurdie H. F. *Phase Diagrams for Ceramists*. Ohio: American. Ceramic Society; 1964. 600 p.

8. Berezhnoi A. S. *Mnogokomponentnyye sistemy okislov* [Multicomponent systems of oxides]. Kiev: Naukova dumka Publ.; 1970. 542 p. (In Russ.)

9. Toropov N. A., Barzakovsky V. P., Lapshin V. V., Kurtseva N. N. *Diagrammy sostoyaniya silikatnykh sistem. Spravochnik. Vyp. pervyy. Dvoynyye sistemy* [State diagrams of silicate systems. Reference book. Issue first. Binary systems]. Leningrad: Science, Leningrad Branch Publ.; 1969. 822 p. (In Russ.)

10. Jung I. -H., Decterov S. A., Pelton A. D. Critical thermodynamic evaluation and optimization of the MgO-Al_2O_3, CaO-MgO-Al_2O_3, and MgO-Al_2O_3-SiO_2 systems. *Journal of Phase Equilibria and Diffusion*. 2004;25(4): 329–345. https://doi.org/10.1007/s11669-004-0151-4

11. Zienert T., Fabrichnaya O. Thermodynamic assessment and experiments in the system MgO-Al_2O_3. CALPHAD. 2013;40: 1–9. https://doi.org/10.1016/j.calphad.2012.10.001

12. Lea F. M., Desh C. H. *The chemistry of cement and concrete*. 2d ed., London: Edward Arnoid & Co; 1956.

13. Nurse R. W., Welch J. H., Majumdar A. J. The CaO-Al_2O_3 system in a moisture-free atmosphere. *Transactions of the British Ceramic Society*. 1965;64: 409–418.

14. Berman R. G., Brown T. H. *A* Thermodynamic model for multicomponent melts, with application to the system CaO-$A1_2O_3$-SiO_2. *Geochimica et Cosmochimica Acta*. 1984;48(4): 661–678. https://doi.org/10.1016/0016-7037(84)90094-2

15. Mao H., Selleby M., Sundman B. A re-evaluation of the liquid phases in the CaO-Al_2O_3 and MgO-Al_2O_3 systems. *CALPHAD*. 2004;28(3): 307–312; https://doi.org/10.1016/j.calphad.2004.09.001

16. Jerebtsov D. A., Mikhailov G. G. Phase diagram of CaO-Al_2O_3 system. *Ceramics International*... 2001;27(1): 25–28. https://doi.org/10.1016/S0272-8842(00)00037-7

17. Smirnov G. S., Chatterjee A. K., Zhmoidin G. I. The phase equilibrium diagram of the ternary subsystem CaO-CaO·Al_2O_3-11CaO·$7Al_2O_3$·CaF_2. *Journal of Materials Science*. 1973;8(9): 1278–1282. https://doi.org/10.1007/BF00549342

18. Taylor H. F. W. *Cement chemistry*. London: Thomas Telford; 1997. 459 p.

19. Lea F. *Lea's chemistry of cement and concrete*. London: Elsevier Ltd; 1998. 1057 p.

20. De Noirfontaine M. -N., Tusseau-Nenez S., Girod-Labianca C., Pontikis V. CALPHAD formalism for portland clinker: Thermodynamic models and databases. *Journal of Materials Science*. 2012;47(3): 1471–1479. https://doi.org/10.1007/s10853-011-5932-7

21. Hentschel G. Mayenit $12CaO{\cdot}7Al_2O_3$ und brownmillerit, $2CaO{\cdot}(Al,Fe){\cdot}2O_3$, zwei neue minerale in den kalksteineinschlüssen der lava des ettringer bellerberges. *Neues Jahrbuch für Mineralogie, Monatshefte*. 1964: 22–29.

22. Tolkacheva A. S., Shkerin S. N., Plaksin S. V., et al. Synthesis of dense ceramics of single-phase mayenite ($Ca_{12}Al_{14}O_{32}$)O. *Russian Journal of Applied Chemistry*. 2011;84(6): 907–911. https://doi.org/10.1134/S1070427211060012

23. Rankin G. A., Merwin H. E. The ternary system CaO-Al_2O_3-MgO. *Journal of the American Chemical Society*. 1916;38(3): 568–88; https://doi.org/10.1021/ja02260a006

24. De Aza A. H., Iglesias J. E., Pena P., De Aza S. Ternary system Al_2O_3–MgO–CaO: Part II, Phase relationships in the subsystem Al_2O_3-$MgAl_2O_4$-$CaAl_4O_7$. *Journal of the American Chemical Society*. 2000;83(4): 919–27. https://doi.org/10.1111/j.1151-2916.2000.tb01295.x

Information about the authors

Vera P. Vorob'eva, DSc in Physics and Mathematics, Leading Researcher at the Sector of Computer Materials Design, Institute of Physical Materials Science, Siberian Branch of the Russian Academy of Sciences, Ulan-Ude, Russian Federation; e-mail: vvorobjeva@mail.ru. ORCID iD: https://orcid.org/0000-0002-2714-3808.

Anna E. Zelenaya, PhD in Physics and Mathematics, Senior Researcher at the Sector of Computer Materials Design, Institute of Physical Materials Science, Siberian Branch of the Russian Academy of Sciences, Ulan-Ude, Russian Federation; e-mail: zel_ann@mail.ru. ORCID iD: https://orcid.org/0000-0001-5232-8567.

Vasily I. Lutsyk, DSc in Chemistry, Head of the Sector of Computer Materials Design, Institute of Physical Materials Science, Siberian Branch of the Russian Academy of Sciences, Ulan-Ude, Russian Federation; e-mail: vluts@ipms.bscnet.ru. ORCID iD: https://orcid.org/0000-0002-6175-0329.

Marina V. Lamueva, post-graduate student of Sector of Computer Materials Design, Institute of Physical Materials Science SB RAS, Ulan-Ude, Russian Federation, e-mail: marina_bgu@mail.ru. ORCID iD: https://orcid.org/0000-0001-8347-1753.

Received 31 May 2021; Approved after reviewing 23 June 2021; Accepted for publication 15 July 2021; Published online 25 September 2021.

Translated by Irina Charychanskaya
Edited and proofread by Simon Cox